



A multifunctional display based on photo-responsive perovskite light-emitting diodes

In the format provided by the authors and unedited

Table of contents

Supplementary Fig. 1: Electroluminescence performance of red LEDs with different amounts of 5AVAI. (page 2)

Supplementary Fig. 2: The angular distribution of the EL intensity of the red PeLEDs. (page 3)

Supplementary Fig. 3: Photoluminescence quantum efficiencies of CsPbI_{3-x}Br_x emitters with different amounts of 5AVAI. (page 4)

Supplementary Fig. 4: Statistics of EQE (electricity to light conversion) and PCE (light to electricity conversion), and stability of our perovskite devices. (page 5)

Supplementary Fig. 5: The waveforms of the light emitted from the PeLED under square function drive voltage. (page 6)

Supplementary Fig. 6: J-V curves of photo-responsive red LEDs based on CsPbI_{3-x}Br_x emitters with different amounts of 5AVAI when working as solar cells. (page 7)

Supplementary Fig. 7: EQE spectrum of the perovskite device working at the PV mode and the radiance spectrum of the commercial LED lamp. (page 8)

Supplementary Fig. 8: Noise current spectrum of the photo-responsive perovskite LED. (page 9)

Supplementary Table 1: Performance of some typical fast-response solution-processed photodetectors. (page 10)

Supplementary Fig. 9: The falling time fitted from the transient photocurrent curves of devices with different device areas. (page 11)

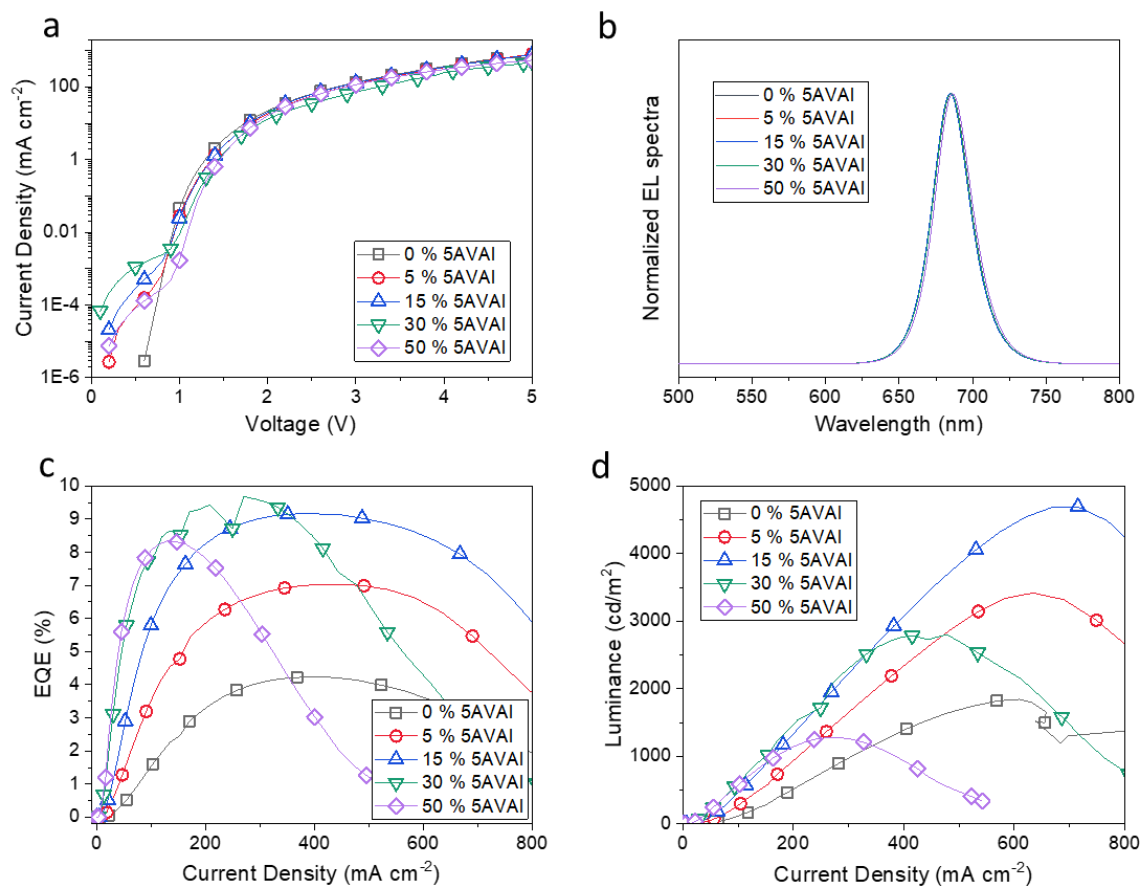
Supplementary Fig. 10: Schematic structure of the proof-of-concept display based on PeLEDs. (page 12)

Supplementary Fig. 11: Electroluminescence and photo-response performance of green and blue photo-responsive PeLEDs. (page 13)

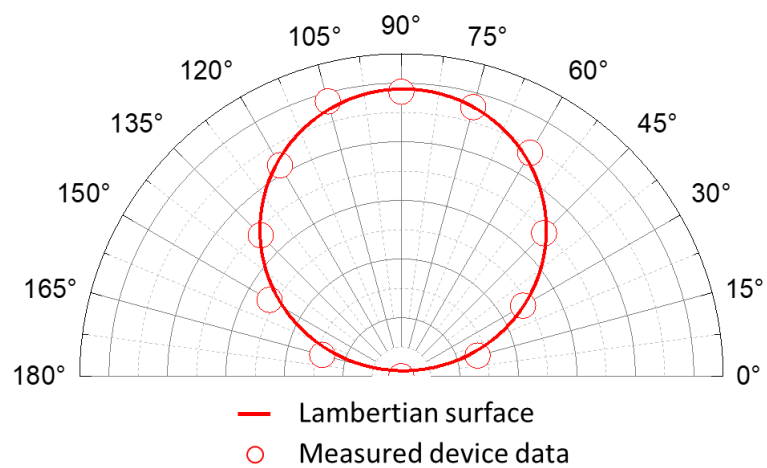
Supplementary Table 2 Electroluminescence and photo-response performance of red, green and blue photo-responsive PeLEDs. (page 14)

Supplementary Fig. 12: Images and PPG signals of a commercial PPG sensor and our multifunctional perovskite display. (page 15)

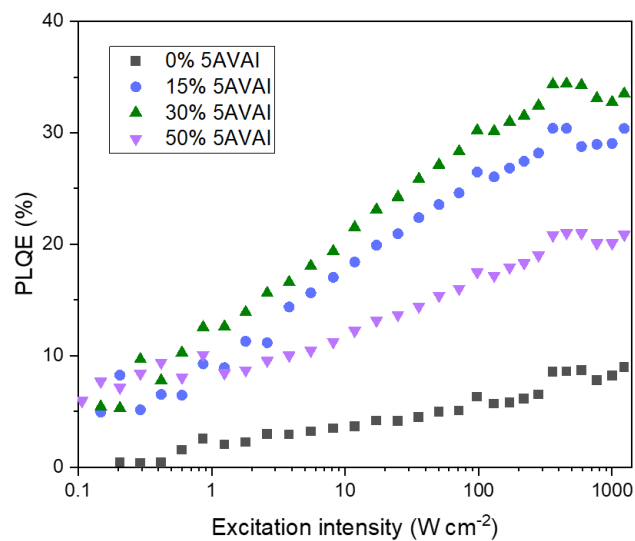
Supplementary Fig. 13: Circuit diagram of the control unit of the PM display demonstration system. (page 16)



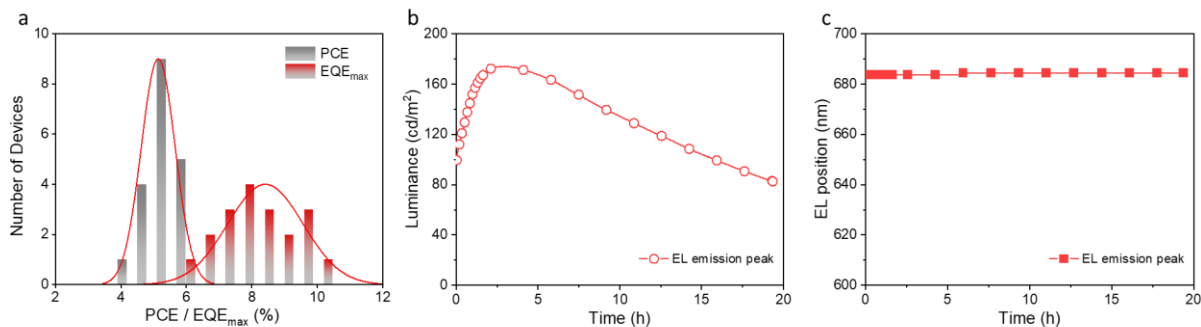
Supplementary Fig. 1: Electroluminescence performance of photo-responsive red LEDs based on $\text{CsPbI}_{3-x}\text{Br}_x$ emitters with different amounts of 5AVAI. a. current density-voltage (J - V) curves, **b.** normalized emitting spectra, **c.** current density dependent EQE (EQE - J) curves and **d.** current density dependent luminance (L - J) of the perovskite LEDs with different additive amounts.



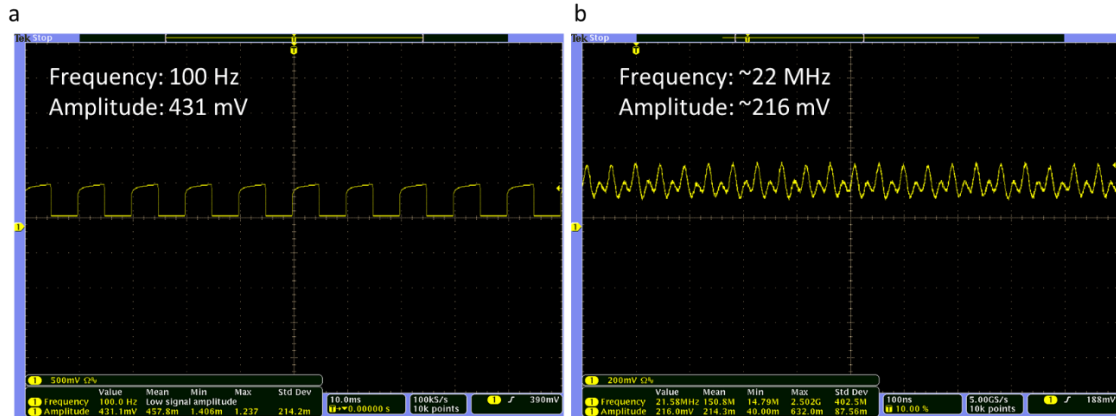
Supplementary Fig. 2: The angular distribution of the EL intensity of our red PeLEDs.



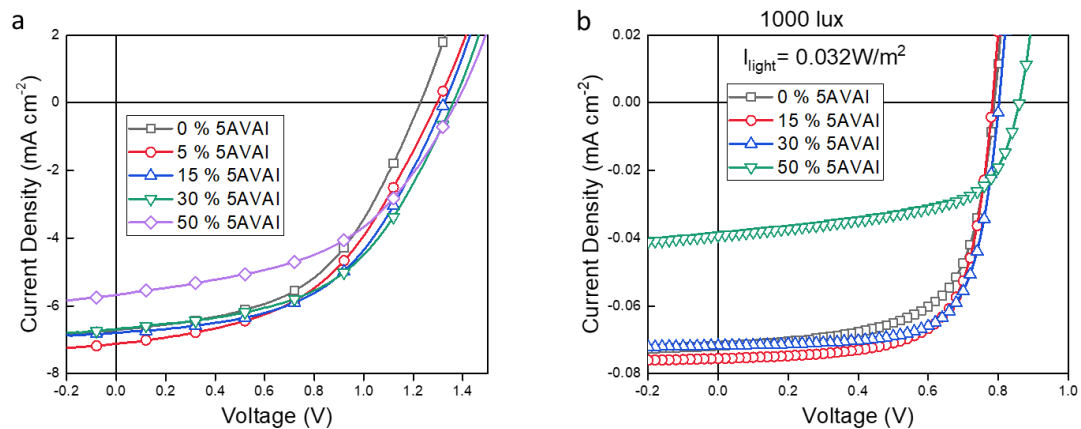
Supplementary Fig. 3: (a) Photoluminescence quantum efficiencies (PLQEs) of CsPbI_{3-x}Br_x emitters with different amounts of 5AVAI.



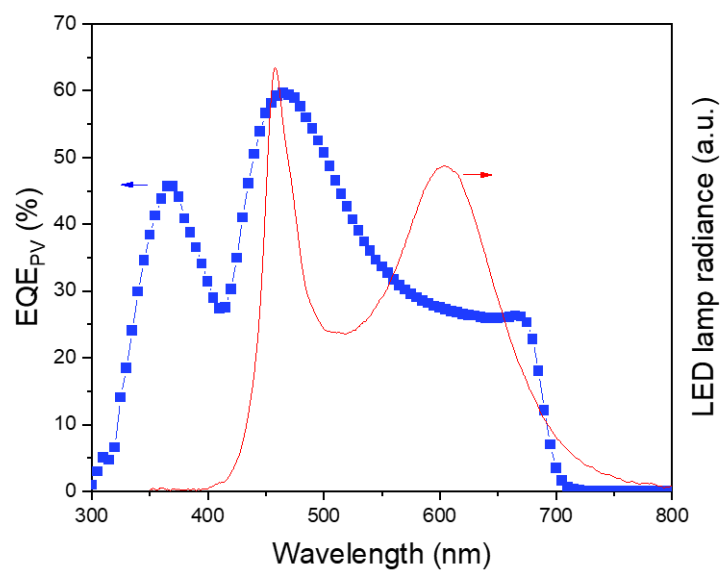
Supplementary Fig. 4: Statistics of EQE (electricity to light conversion) and PCE (light to electricity conversion), and stability of our perovskite devices. a. maximum EQE and PCE histogram of multifunctional devices functioning as LEDs and solar cells respectively. The totally number of the pixels is 20. **b.** operational stability of PeLEDs emitting in red color. The initial brightness is 100 Cd m⁻². **c.** peak position of the EL emission spectra during the operational stability measurement.



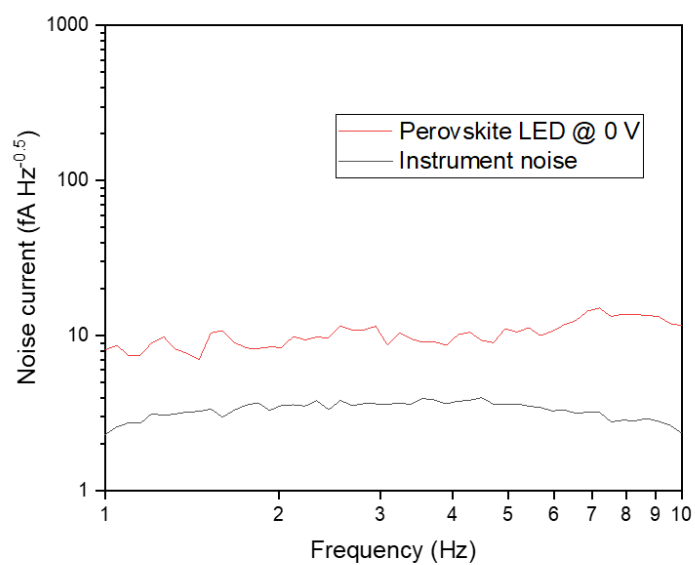
Supplementary Fig. 5: The waveforms of the light emitted from the PeLED with a device area of 0.2 mm² driven by a square-wave drive voltage with 100 Hz (**a**) and 22 MHz (**b**).



Supplementary Fig. 6: J-V curves of photo-responsive red LEDs based on CsPbI_{3-x}Br_x emitters with different amounts of 5AVAI when working as solar cells under illumination from the AM1.5G solar simulator (a) and 1000 lux white LED (b).



Supplementary Fig. 7: EQE spectrum of the perovskite device working at the PV mode and the radiance spectrum of the commercial LED lamp used as light source for indoor-light PV performance measurement.



Supplementary Fig. 8: Noise current spectrum of the photo-responsive perovskite LED when working at zero bias as a photodetector, and the noise baseline of the test instrument.

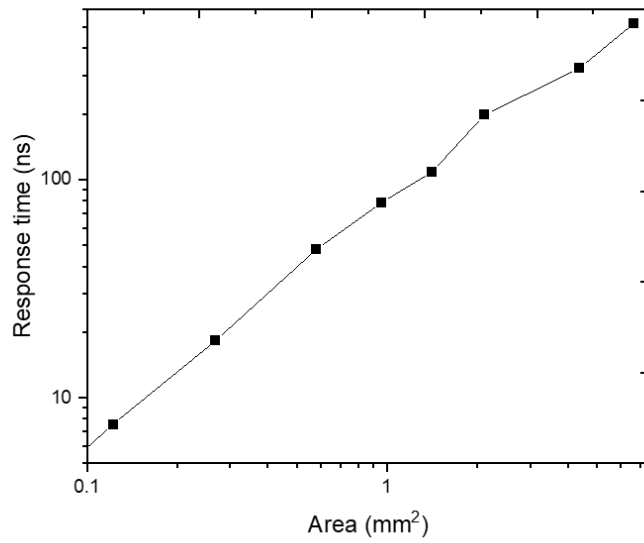
Supplementary Table 1: Performance of some typical fast-response solution-processed photodetectors.

Absorber	D*(Jones)	f _{-3dB}	t _{fall} (ns)	Area (mm ²)	Bias (V)	Reference
Organic	8×10 ¹²	15kHz	--	11	--	<u>Science, 2020, 370, 698</u>
Organic	5.6×10 ¹¹	2MHz	--	2.5	--	<u>Adv. Func. Mater., 2019, 1808948</u>
Organic	2.52×10 ¹¹	1.7MHz	289	--	-1	<u>Small, 2017,1603260</u>
CdSe CQD	1×10 ⁷	50 kHz	--	1.22	--	<u>Appl. Phys. Lett. 2005, 87, 213505</u>
PbS CQD	1×10 ¹²	3 MHz	--	1.96	-5	<u>Nat. Nanotech., 2009, 4, 40</u>
Perovskite	7.8×10 ¹²	168 MHz ^a	0.95	0.04	0	<u>Adv. Mater.2016, 28, 10794</u>
Perovskite	5.3×10 ¹²	65 MHz ^b	3.86	0.1	0	<u>Nat. Electron., 2020, 3, 156</u>
Perovskite	1.5×10 ¹²	1.6 GHz ^a	0.1 ^c	10 ⁻⁴	0	<u>Nat. Electron. 2022, 5, 511</u>
Perovskite	6.08×10 ¹²	142 MHz ^b	3.83 ^c	0.06	0	This work

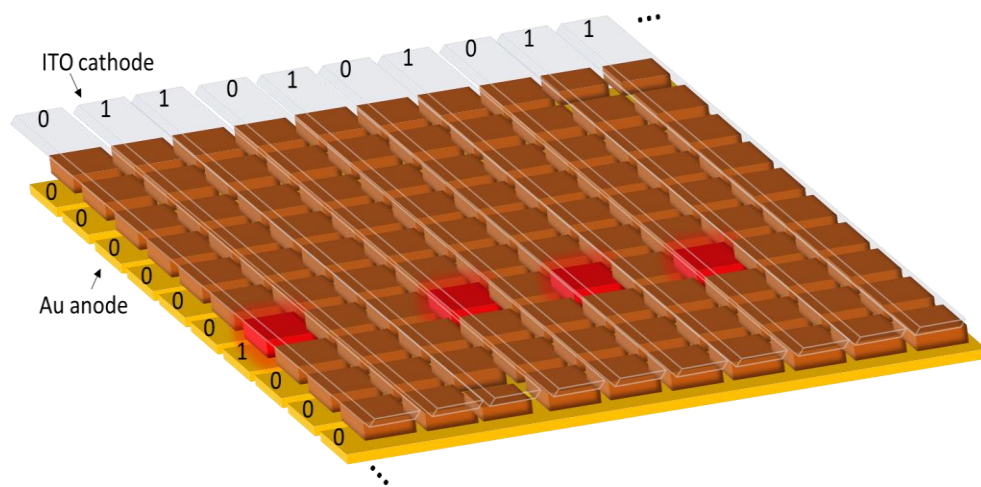
^a calculated from fall time using $f_{-3dB} = (2\pi RC)^{-1}$

^b obtained from the FFT of the TPC curve

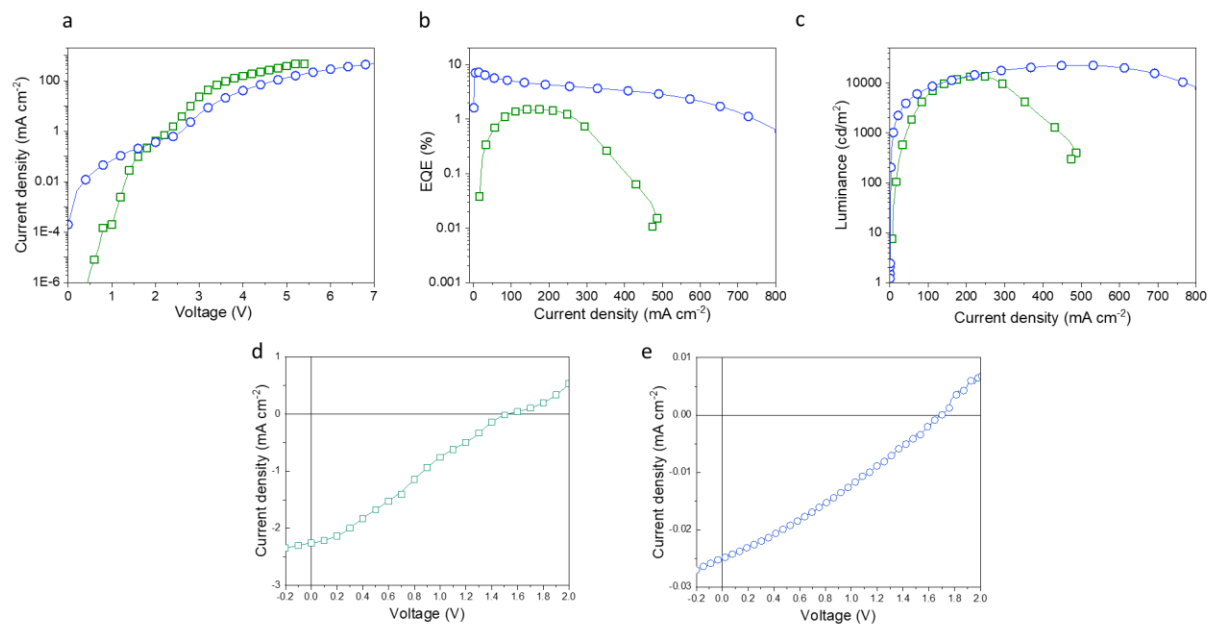
^c full-width at half-maximum of the TPC curve



Supplementary Fig. 9: The falling time fitted from the transient photocurrent curves of devices with different device areas.



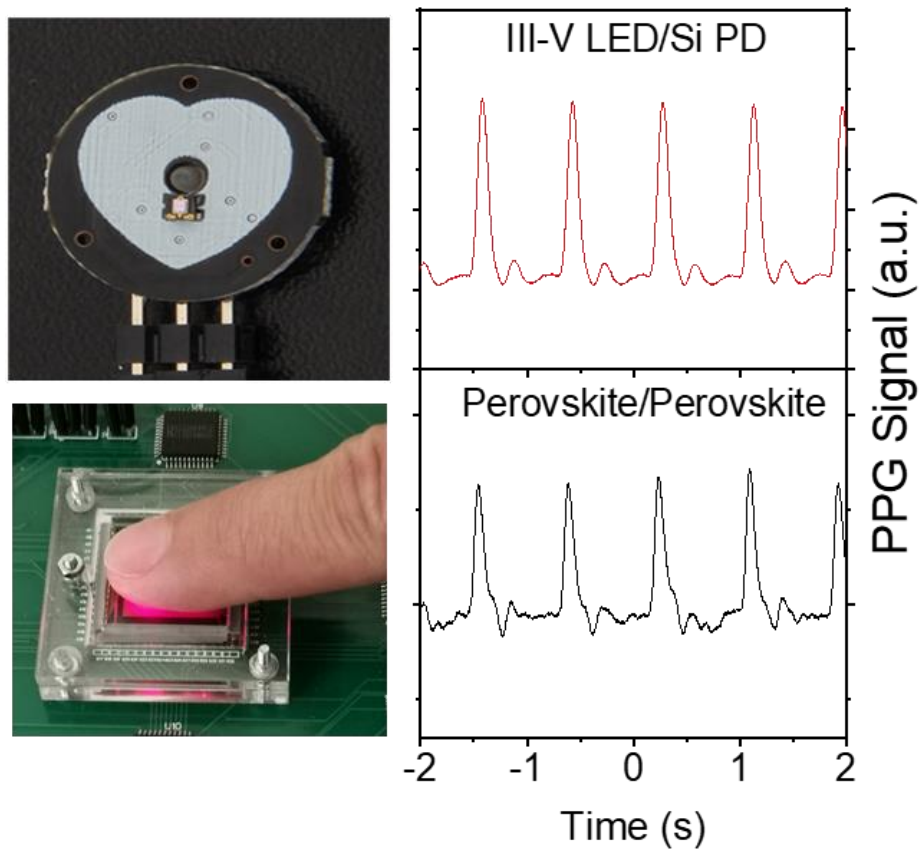
Supplementary Fig. 10: Schematic structure of the proof-of-concept display based on PeLEDs.



Supplementary Fig. 11: Electroluminescence and photo-response performance of green and blue photo-responsive PeLEDs. a. J-V curves under the forward bias, **b.** EQE-current density curves; **c.** Luminance-current density curves. **d** and **e.** J-V curves of PeLEDs under the AM1.5G conditions. The green line and blue line represent PeLEDs emitting at green and blue region.

Supplementary Table 2: Electroluminescence and photo-response performance of red, green and blue photo-responsive PeLEDs.

Color	Device structure	LED mode		Solar cell mode			
		EQE _{EL} (%)	Luminance (cd m ⁻²)	V _{OC} (V)	J _{SC} (mA cm ⁻²)	FF (%)	PCE (%)
Red	ZnO/CsPbI _{3-x} Br _x /TFB	9.7	4700	1.33	7.9	51	5.34
Green	ZnO/FAPbBr ₃ /TFB	1.5	13834	1.53	2.3	28	0.98
Blue	PTAA/2PACz/PVP/CsPbBr _{3-x} Cl _x /TPBi	7.4	22749	1.7	0.025	28	0.012



Supplementary Fig. 12: Images of a commercial PPG sensor based on III-V LED and Si photodiode (top) and multifunctional perovskite display working as PPG sensor (bottom), as well as the corresponding PPG signals.

